Fusion Engineering and Design 191 (2023) 113585

Contents lists available at ScienceDirect

Fusion Engineering and Design

journal homepage: www.elsevier.com/locate/fusengdes

Structural analysis of the ex-port plug collective thomson scattering transmission lines for ITER

E. Rincón [a,*], E. Blanco [a], M. Medrano [a], J. Imaz [b], Y. Villalobos [b], L. Maldonado [b], P. Varela [c], Y. Liu [d], V. Udintsev [d]

[a] CIEMAT. Laboratorio Nacional de Fusión. Avda. Complutense 40, Madrid 28040, Spain
[b] EMPRESARIOS AGRUPADOS, Magallanes 3, Madrid 28015, Spain
[c] Instituto de Plasmas e Fusão Nuclear, IST, Universidade de Lisboa, Lisboa 1049-001, Portugal
[d] ITER Organization, Route de Vinon, St Paul-lez-durance 13067, France

ARTICLE INFO

Keywords:
ITER
CTS
Diagnostic
Structural analysis
FEM
RCC-MR

ABSTRACT

The main function of the Collective Thomson Scattering (CTS) diagnostic system for ITER is to diagnose the alpha particles resulting from Deuterium-Tritium fusion reactions. It consists of a microwave scattering diagnostic with a probing frequency of 60 GHz and emitted power of 1.2 MW from the gyrotron, with one launcher and nine receiver transmission lines.

The CTS will be installed in the equatorial port EP#12, which is one of the ports that have to be operational for the ITER First Plasma. The transmission lines outside the Port Plug (Ex-PP) are routed through the Interspace, Port Cell, Gallery, Assembly Building and Diagnostic Building, reaching more than 100 m in length. The preliminary design of the ex-PP components is currently being undertaken in the framework of an Implementing Agreement between ITER Organization, the Instituto Superior Técnico (IST) and CIEMAT. Within this collaboration, CIEMAT is responsible for the structural analyses and calculations required to ensure the structural integrity and performance of the preliminary design of the Ex-PP transmission line components, which will be summarized in this paper.

In this work, the required analysis and calculations will be presented together with the redesign performed for the transmission lines in order to guarantee that their components will withstand the loads defined in the Ex-PP CTS Load Specifications. The evaluation of the structural integrity of the CTS Ex-PP components will be carried out in accordance with the 2007 RCC-MR Code for mechanical components in nuclear installations.

1. Introduction

The Collective Thomson Scattering (CTS) in ITER is a microwave diagnostic system intended to monitor the ITER plasma. The aim of CTS is to provide measurement of plasma parameters related to the ion velocity distribution function, in particular of fast ions. The diagnostic is based on the collective Thomson scattering principle of a powerful mm-wave beam of electrons in the plasma. The radiation scattered in specified directions provides information on the fast ions [1].

The CTS diagnostic in ITER consists of one launcher and nine receiver transmission lines (TLs). The front-end launcher and receiver components, integrated into the Diagnostic Shield Module 3 of the Equatorial Port Plug 12 (EPP12), are intended to launch the probe beam into a suitable direction in the plasma and to collect radiation on an array of receiver mirrors and horns. The function of the launcher TL is to transmit the high power beam from the gyrotron millimeter-wave source (60 GHz, 1.2 MW) to the front end, while the receiver TLs transmit the low power signals received in the front end to the data acquisition and processing electronics located at the back-end.

This work is focused on the TLs located outside the Port Plug (Ex-port plug), with a total length of 100 m, distributed as follows (Fig. 1):

- The Ex-port plug Launcher TL is routed from the gyrotron in the Assembly Building 13 (B13), through the Gallery, Port Cell (PC) and Interspace (IS) in Building 11 (B11), to the closure plate of the EPP12.

* Corresponding author.
E-mail address: esther.rincon@ciemat.es (E. Rincón).

https://doi.org/10.1016/j.fusengdes.2023.113585
Received 10 October 2022; Received in revised form 20 December 2022; Accepted 16 February 2023
Available online 21 February 2023

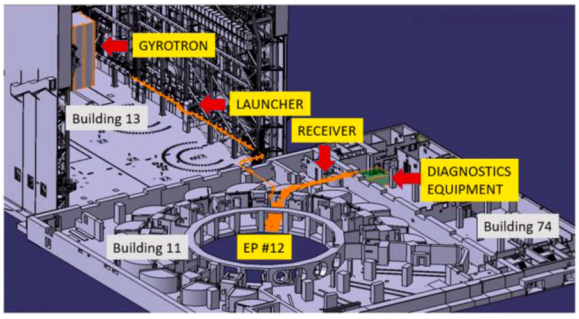

Fig. 1. CTS general layout.

- The Ex-port plug Receiver TLs are routed in B11 from the closure plate of the EPP12, through the IS, PC and Gallery, to the electronics cubicles located in the Diagnostic Building (B74).

This document summarizes the thermo-mechanical analyses and calculations required in the preliminary design of the CTS Ex-port plug TLs, as well as the redesign performed as a result of these calculations, to guarantee both the structural integrity and the microwave transmission performance of the diagnostic.

Assessment on the structural integrity of the CTS Ex-Vessel components is made in accordance with the RCC-MR 2007 Code for mechanical components of nuclear installations [13].

2. Scope

The components under the scope of this work are the Ex-port plug transmission lines defined in Section 1, with all the attached components defined in Section 3.

Although the structural integrity assessment of the supports, secondary windows and firebox structures, are not in the scope of this work, they have been included in the model to obtain a proper simulation of the boundary conditions.

However, since the design of the CTS is at the Preliminary stage, the components attached to the transmission lines, such as the miter bends, sliding joints, or the Zero gravity support, have been simplified in the global model. They have been modeled only to take into account their effect on the TLs in terms of applied weight, boundary conditions of degrees of freedom. But the detailed analysis of these components will be carried out when they are defined in the later stages of the CTS design.

Regarding the applied loads, only those defined in Section 4 have been taken into account in this work. However, thermal loads due to the microwave ohmic losses in the Launcher line will also be analyzed in the later stages of the CTS design, in order to check the cooling performance, as well as the temperature distribution and deformations in the main components.

3. System description

The CTS Ex-port plug Launcher and Receiver TLs consist of straight sections of oversized circular corrugated waveguides. All the components in the Launcher TL are water-cooled to minimize their thermal expansion due to the heating caused by the power losses. Besides, the launcher TL is connected to the ITER vacuum system to prevent the arcing and avoid additional losses due to O_2 absorption. The design and integration of the components and the cooling pipes in the Launcher TL are similar to those adopted in the ITER ECRH (Electron Cyclotron Resonance Heating) system, since the gyrotron output power and TLs are very much alike in both systems, apart from the waveguide dimensions [2-5].

The main components of the Ex-port plug TLs are described below:

3.1. Waveguide (WG) section

The straight waveguide sections have an internal diameter of ∅88.9 mm for the Launcher TL and ∅63.5 mm for the Receiver TLs, with a maximum length of 2 m. Most of the waveguide sections are made of aluminum Al 6061-T6, except where stainless steel (SS 316 L) is required for safety and structural integrity reasons. Waveguides in the Launcher TLs include four cooling pipes running along the waveguide length, with an inner diameter of ∅16 mm (Fig. 2).

3.2. Waveguide flanges and couplings

The function of the waveguide flanges and couplings is to connect and align the guides to each other or to other TL component. Flanges are machined at both ends of the Launcher waveguide sections, and include a metallic seal to ensure the vacuum that the waveguides have to withstand. On the other hand, the couplings in the Receiver TLs are designed to provide the alignment precision required to minimize mode conversion losses. Long couplings are used when possible, since they provide a more rigid connection, but short couplings have to be used when there are space restrictions (Fig. 3).

3.3. Miter bends (MB)

Miter bends are installed to redirect the propagation of the microwave beam by means of the miter bend mirror. All the miter bends are 90°, except one miter bend in the Launcher TL, located in the Gallery, which is 140°. Miter bends in the Receiver TLs are made of Al 6061-T6, except in the locations where SS 316 L is required due to safety and structural integrity reasons. However, all the miter bends in the Launcher TLs are made of CuCrZr, with four cooling channels of ∅16 mm, to avoid thermal deformation of the mirror surface (Fig. 4).

3.4. Sliding joints (SJ)

The sliding joints allow differential axial movements of the TL components, to avoid the stresses due to thermal expansion loads. As in the miter bends, the sliding joints are made of Al 6061-T6 and SS 316 L in the Receiver TLs. But in the Launcher TL they are made of CuCrZr, with four cooling channels (two at each side) of ∅10 mm to avoid thermal deformations in the sliding area, and welded bellows with metal seals to ensure the vacuum inside the expansion unit (Fig. 5).

4. Applied loads

The loads and load combinations applied in the Structural analysis are compliant with the Load Specifications approved by ITER for the CTS components in Building 13 [6], Gallery [7], Interspace and Port Cell [8], and Diagnostic Building 74 [9].

The main loads to be taken into account include Gravity, Seismic events, Electromagnetic (EM) loads due to transient events, Thermal loads, and Loads in incident and accidental events.

- **Gravity** acceleration is applied to the 1950 kg mass of the Receiver and 3500 kg mass of the Launcher Ex- Port plug TLs.
- **Seismic Events** corresponding to Level 1 (SL-1), SMHV (Maximum historically probable earthquake), Level 2 (SL-2), and Level 3 (SL-3),

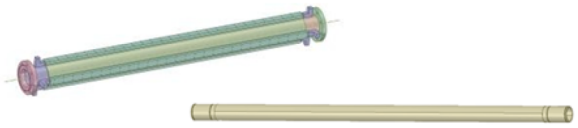

Fig. 2. Waveguide section for the Launcher TL (on the left) and Receiver TL (on the right).

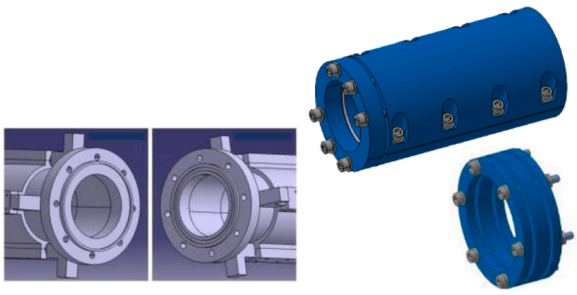

Fig. 3. Waveguide flanges (on the left) and couplings (on the right).

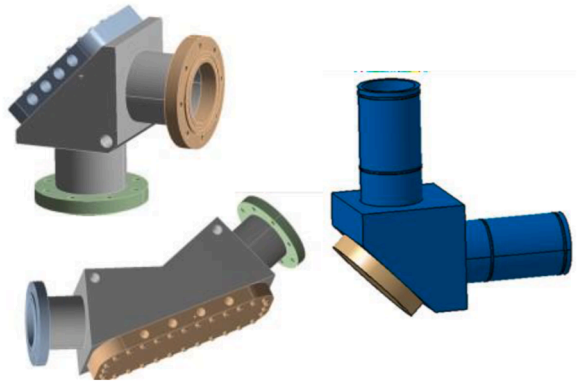

Fig. 4. Miter bends for the Launcher TL (on the left) and Receiver TL (on the right).

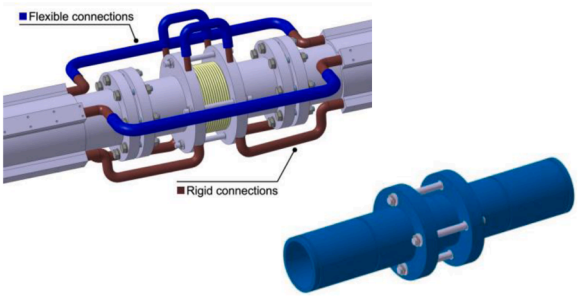

Fig. 5. Sliding joints for the Launcher TL (on the left) and Receiver TL (on the right).

have to be considered, according to the seismic and safety classification of the components in each area, as defined in [9] for the B13, in [10] for the Gallery, in [11] for the IS and PC, and in [12] for the B74. Multispectral analysis is performed applying the corresponding Response Spectra to the waveguide supports, with a damping factor of 3% for all the seismic levels.

- **EM loads** due to transient events can be considered negligible for the components located outside the Bioshield, according to the values of dB/dt provided in [14] and [15]. For the EM loads inside the Bioshield, an EM analysis has been performed on the ISS of EPP12, including the CTS TLs [16]. The stresses obtained on the CTS TLs due to the volumetric forces calculated in the EM Analysis result to be lower than 2 MPa, proving that the influence of the EM loads is also negligible for the Ex-PP TLs inside the Bioshield.
- **Thermal load** during normal operation is assumed to be a uniform temperature that ranges from 5 °C to 35 °C in the Gallery, PC and IS. For the Assembly Building 13 and Diagnostic Building 74, temperature varies between 18 °C and 27 °C. Extra heating due to nuclear loads is considered negligible outside the Port plug.
- **Loads in incident and accidental events** include Loss of Coolant (LOCA) and Internal Fire events.

  - The only LOCA event that is expected to affect the Ex-Port plug TLs is the LOCA in the Port Cell, resulting in a uniform temperature of 145 °C in the IS and PC, and 60 °C in the Galleries. Diagnostic Building 74 and the Assembly Building 13 are not affected by the ex-vessel LOCA events.
  - Regarding the Internal Fire, a maximum temperature of 200 °C is considered for fire protected components, while 400 °C is applied to non-protected Aluminum TLs in the ISS (Interspace Support Structure) and PCSS (Port Cell Support Structure) to evaluate their displacements and forces induced until melting temperature is reached. Al TLs are assumed to reach the melting point at 400 °C, without damaging other Safety Important Components.

- **Interface Loads** are also applied in the ISS and PCSS, for the seismic and fire events, to take into account the relative displacements between the CTS TL supports.

Table 1 summarizes the enveloped load combinations (LC) applied in the analyses for every Load Category, according to [6-8] and [9], and taking into account all the above considerations.

5. Structural analyses

5.1. Methodology

Two independent global models have been performed for the thermo-mechanical analyses: one for the entire Receiver Ex-Port plug TL, which includes in one single model the nine transmission lines in all areas, from the MOU (Matching Optics Unit) in the ISS to the B74 cubicles; and the other for the Launcher Ex-Port plug TL, also from the MOU in the IS, but to the gyrotron in B13.

First, an assessment has been made for the fire event, in order to detect excessive loads on the transmission lines due to the boundary conditions (BC), which would imply high reaction loads on the supports with the consequent risk of failure. The reason to start with an assessment of the fire event is to correctly define the waveguide supports and expansion joints, so ensuring that the largest expansion of the transmission lines will not cause any damage to the hard core components, where Normal damage is also required for Category IV loads.

Once the BC are adjusted to get a balanced load on the supports, seismic events are evaluated by means of a multipoint Spectral analysis, followed by independent Structural Analyses for each one of the individual loads described in Section 3. And finally, the results obtained for each individual load are combined as per each load combination listed in Table 1.

The objective of the above analyses is to assess the structural integrity of the CTS Ex-Port plug TLs in their preliminary design stage, and to

Table 1
Load combinations to be applied at PDR stage.

Cat.	Initiating event	Concat. event
I	I.2. Gravity + Thermal+ EM	
II	II.11. Gravity + Thermal + Seismic (SL1) + SL1_interface + EM	
III	III.19. Gravity + LOCA in GalleryIII	
	III.20. Gravity + LOCA in PC	
	III.25. Gravity + Thermal + Seismic (EC8/SMHV) + SMHVinterface	
IV	IV.13. Gravity + Thermal+ Seismic (SL2) + SL2 interface	
	IV.13. Gravity + Thermal + Seismic (SL2) + SL2 interface	Fire in Gallery &PC
V	Scenario 11. Gravity + Thermal + Seismic (SL3 in Gallery)	

ensure that the deformations in normal operation are within the acceptable tolerances.

According to RCC-MR, in order to isolate the primary stresses to assess P-type damage when thermal loads are applied, the thermal expansion coefficient has been set to zero in the material properties, so that the resulting stresses do not include the secondary ones coming from internal loadings, but only the primary stresses coming from external mechanical loads.

In addition to the above Structural Analyses, a Modal Analysis has also been performed to evaluate the natural frequencies of the Ex-port plug TLs.

5.2. Finite element model (FEM)

The analysis has been performed with ANSYS Workbench 19.2.

The coordinate system used in the FEM analysis is the Cartesian Tokamak Global Coordinate System (TGCS), with the origin in the center of the ITER torus, the Z-axis in the vertical direction and the X-axis in radial direction at the mid plane of the Toroidal Field Coil 01.

The mesh in the FEM is mostly composed of beam elements BEAM188 for the supports and PIPE289 for the waveguides. Solid elements SOLID185 of 3D hexahedral 8-node have been used for the simulation of the filling material in the penetrations. MASS21 elements are used to represent the weights of the sliding joints, miter bends couplings, flange connections, secondary windows, valves, vacuum pump, dc-break and MOUs. And Quadrilateral 8-node surface elements TARGE 174 and CONTA170 have been used for contact simulation. Element size has been reduced to get the highest quality mesh within acceptable computing time limits.

An overview of the FEM mesh with all elements modelled is given in Fig. 6 for the Receiver TLs and in Fig. 7 for the Launcher TL.

The model includes several joint connections between different parts of the TLs, with the corresponding restrictions to simulate all the connections in the supports and penetrations, as well as the behavior of the sliding joints.

Fixed boundary conditions are considered for the attachment of the supports to the embedded plates in B13, B74 and ceiling supports in B11. The outer diameter of the filling material in the penetrations is also fixed, as well as the rigid beams for PCSS and ISS Supports. (See Figs. 8 and 9).

In the Launcher TL (Fig. 8), vertical displacements are restricted in the last MB next to the MOU, to take into account the effect of the Zero gravity support, aimed at holding vertical loads coming from the MOU and the lower arm of the TL. Fixed conditions are considered at both ends of the TL, with the MOU and with the gyrotron.

In the Receiver TLs (Fig. 9), vertical displacements are restricted in the base of the support beams in the PCSS, and the nodes are connected to a remote point with the horizontal displacements restricted, so that the support base is not over constrained under thermal expansion, as it is directly connected to the steel base of the PCSS that will be fixed isostatically to avoid thermal stresses. Fixed conditions are considered at the end of the TLs in B74. However, the end of the TLs in the ISS are connected in groups of three with the MOU pending on the waveguides; therefore a remote point has been created to represent the MOU for each group of three TLs.

6. Analysis results

6.1. Modal analysis results

A total of 60 and 62 natural frequencies have been extracted in the Modal Analysis for the Launcher and Receiver TLs, respectively, until 33 Hz is exceeded. As the distance between supports is very small compared to the length of the lines, total mobilized mass under 33 Hz is very low, as shown in the lower line of Tables 2 and 3. Therefore, there are not clearly dominant modes of vibration, as the CTS Layout distribution has several local modes. For the Response Spectrum load cases, Missing Mass Effect ZPA has been activated, in order to accelerate those parts with high frequency ranges >33 Hz.

Tables 2 and 3 summarize the first mode and the three dominant frequencies in each direction for both TLs (Launcher and Receiver). It can be observed that total mobilized mass under 33 Hz is low, due to the small distance between supports and the mass mobilized by the supports themselves.

6.2. Stress results

Primary stresses have been analyzed in the Launcher and Receiver TLs for every Load combination defined Table 1, to assess P-type damage on the Waveguides.

In general, stresses obtained in the Receiver lines are much lower than in the Launcher line, being the most critical area the transition between the PC ceiling and the PCSS. Waveguide supports in this area have been defined to minimize the bending stresses, but still the minimum safety margin is shown in the last support on the ceiling of the PC (see Fig. 10).

As a first conservative simplified approach, the maximum von Mises Primary stress (Svm) obtained for every LC has been compared directly

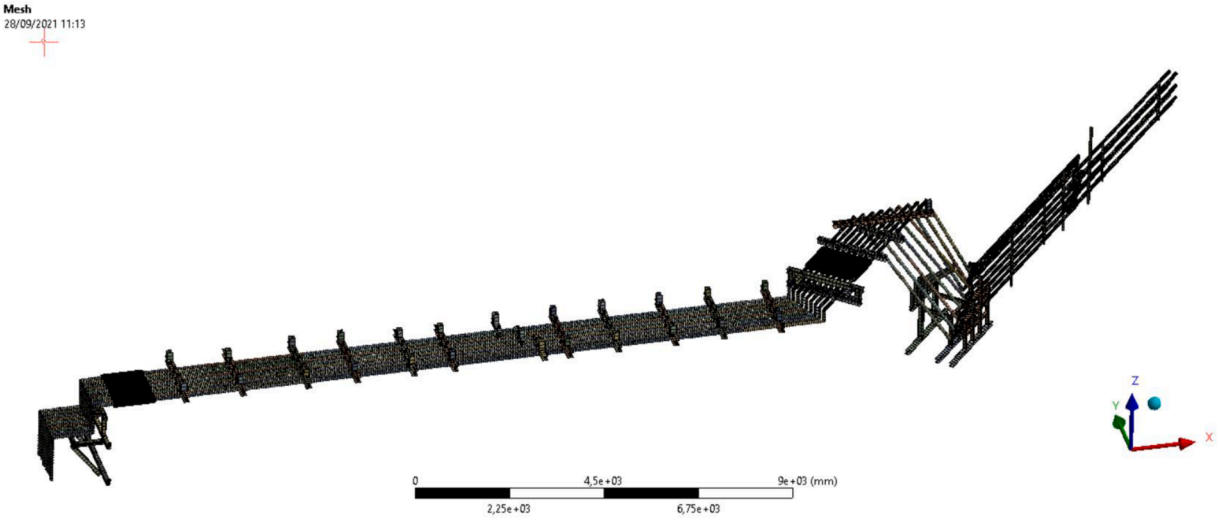

Fig. 6. FEM mesh overview of the CTS Receiver TLs.

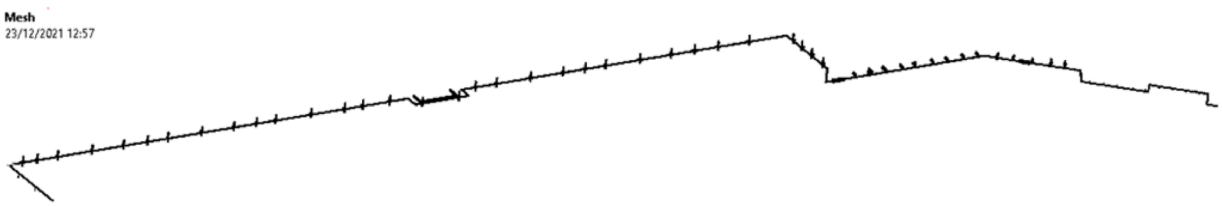

Fig. 7. FE mesh overview of the CTS Launcher TL.

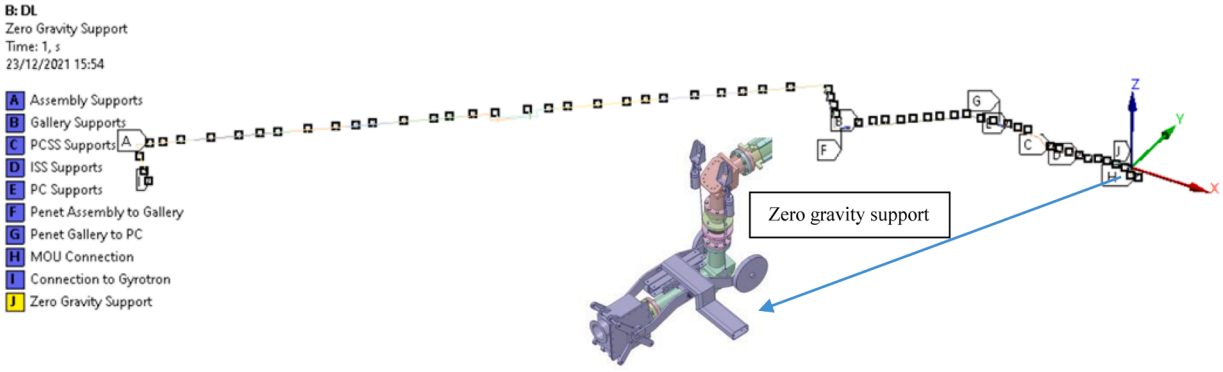

Fig. 8. FEM boundary conditions in the Launcher TL, including a detail of the Zero Gravity Support.

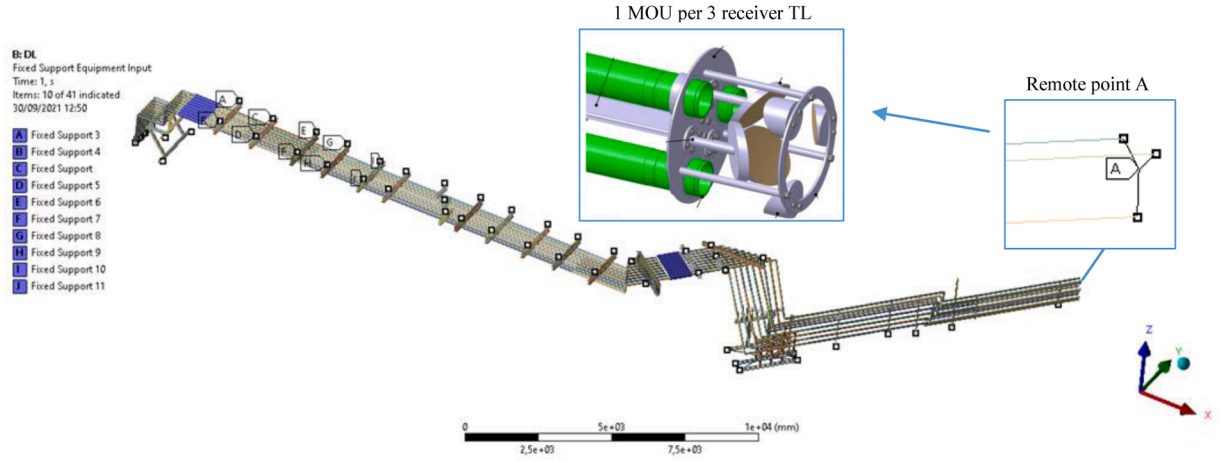

Fig. 9. FEM boundary conditions in the Receiver TLs, including a detail of the MOU connection at the end of the TL.

Table 2
Natural frequencies in the Launcher TL.

Mode	Freq.(Hz)	Effective mass (kg)		
		X-Dir Ratio (%)	Y-Dir Ratio (%)	Z-Dir Ratio (%)
1	3.48	0.027	0.00	0.00
34	24.51	**0.046**	0.01	0.00
18	19.42	0.00	**0.12**	0.00
6	13.39	0.00	0.00	**0.07**
All 60 modes <33Hz		24.53	47.59	27.22

Table 3
Natural frequencies in the receiver TLs.

Mode	Freq. (Hz)	Effective mass (kg)		
		X-Dir Ratio (%)	Y-Dir Ratio (%)	Z-Dir Ratio (%)
1	11.43	0.84	3.71	0.75
5	15.36	0.08	**4.43**	0.01
17	19.48	0.10	1.12	**3.26**
18	19.93	**10.48**	0	0.39
All 62 modes <33Hz		44.45	24.64	16.66

with the maximum allowable stress for every criteria level (Sm), as per RCC-MR [13], without differentiating between membrane and bending, defining the Safety Margin as follows: Safety Margin (Sm) = 1-Svm/Sm

It can be observed in Table 4 that maximum Svm is higher than Sm for load combinations in Category III and IV. Therefore, the conservative approach without differentiating between membrane and bending stresses cannot be applied in these LC. In fact, primary membrane stress is negligible in most sections, due to the sliding joints. Therefore, maximum von Mises stresses shown in Table 4 are mainly Primary bending, so maximum allowable Pm+Pb limit (1.5*Sm) defined in RCC-MR should be applied in for the calculation of the safety margin, according to the following expression:

$$\text{Safety Margin}\,(1.5 * \text{Sm}) \;=\; 1 - (\text{Pm} + \text{Pb}) \,/\, (1.5 * \text{Sm})$$

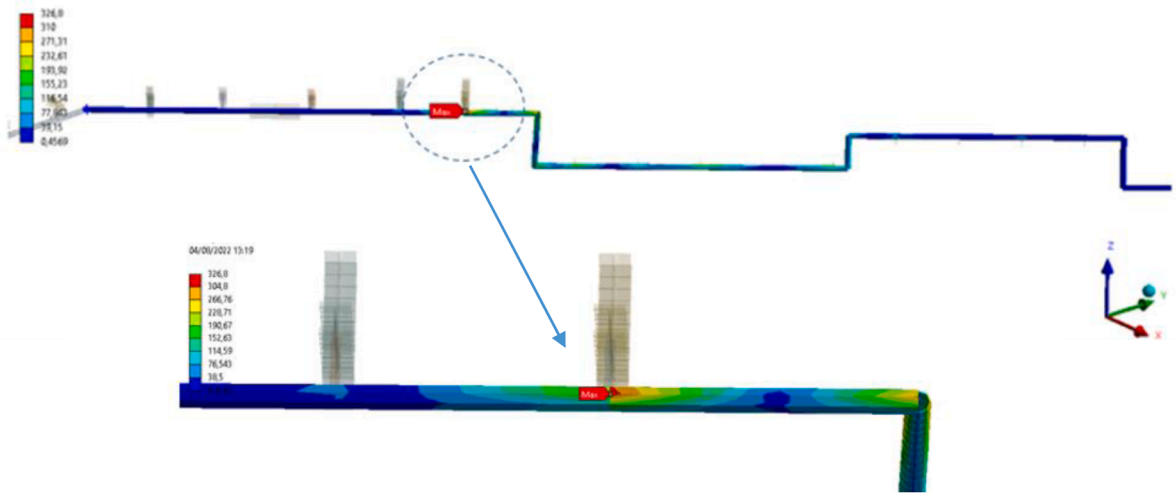

Fig. 10. Maximum Primary stresses for LCIV, showing area with minimum safety margin (transition between PC and PCSS, in Launcher line).

Table 4
Primary stresses with the lowest safety margin per load category.

Cat.	Load Combination	Max. Svm (MPa)	Location	Material	Sm (MPa)	Safety margin (1-Svm/Sm)
I	**I.2.** Gravity +Thermal +EM	21.26	B13 Launcher	Al (Non-SIC/SR)	87.0	0.76
II	**II.11.** Gravity +Thermal +SL1+SL1_interface +EM	66.46	ISS Receiver	Al (Non-SIC)	87.0	0.24
III	**III.25.** Gravity + Thermal + EC8/SMHV + SMHV_interface	130.59	PCSS Launcher	SS (SIC)	127.0	-0,03
IV	**IV.13**. Gravity + SL2 + SL2 interface + Fire + Fire interface	326.80	PC Launcher	SS (SIC)	273.0	-0.20
V	**Scenario 11.** Gravity + Thermal + SL3 in Gallery	46.02	B13 Launcher	Al (Non-SIC)	208.8	0.78

Since the waveguides are defined in the model with PIPE289 elements and the stresses cannot be linearized to calculate the membrane and bending stress, they have calculated from the axial force and bending moment in that section, as shown in Table 5 for the following dimensions of the launcher waveguide section:

Section area, $A = 0.0019\text{m}^2$

Outer radius, $R = 0.0508$ m

Inertia moment, $I = 2.16\text{E-}06\text{m}^4$

Resistant moment, $W = I/R = 4.26\text{E-}05\text{m}^3$

As a result, it can be concluded that maximum primary stresses meet the RCC-MR criteria, since they are below the allowable limits. This confirms the structural integrity of the CTS ex-port plug TLs for P-type damage, so assuring that they will not be subjected to excessive deformation or plastic collapse for any load combination.

6.3. Displacement results

Thermo-mechanical deformations have been analyzed in normal operation, since they could give rise to performance loses. These deformations are mainly driven by Gravity and Thermal loads, due to the variations in the room temperature from 5 °C to 35 °C. Maximum deformations due to Gravity, for 5 °C and 35 °C, are summarized in Table 6.

The maximum transverse displacement occurs mainly due to the self-weight. This displacement is in the order of 8% with respect to the inner WG radius in the Launcher TLs (3.74 mm / 44.45 mm = 8%) and 5% in the Receiver TLs (1.70 mm / 31.75 mm = 5%). Therefore, it is considered acceptable from waveguide performance point of view as it will not induce appreciable micro-wave distortion.

Axial displacements in the direction of the waveguide propagation are absorbed by the sliding joints during operation. The effect of this axial displacement in the microwave performance can be also neglected, since the maximum axial displacements per waveguide length can be estimated as $\Delta L / L = \alpha m\, \Delta T$, with $\Delta T = \pm 15$ °C, and αm as the thermal expansion coefficients for SS and Al, resulting in a maximum value of $\Delta L / L = 0.00034$, which induces a negligible effect on the waveguide corrugations.

On the other hand, thermo-mechanical deformations have also been analyzed under extreme heating conditions like LOCA and Fire events, in order to specify the maximum displacement expected in the sliding joints for those parts that are fire protected. Maximum displacements have been computed at both sides of the sliding joints for LOCA and Fire events. According to the results obtained, two types of SJ have been included for the Launcher TL, with 25 mm and 50 mm range, and other two types for the Receiver TL, with 20 mm and 40 mm range. Maximum displacements reached for each SJ type are summarized in Table 7.

The location of the SJ with the maximum displacement per SJ type is shown in Fig. 11 for the Launcher and in Figs. 12 and 13 for the Receiver.

7. Conclusions

This document covers P-Type damage assessment for the design of

Table 5
Calculation of Primary membrane and bending stresses in the sections showing the lowest safety margin for LC III and IV.

Cat.	LC	Axial Force Fx (N)	Primary membrane Pm=Fx/A (MPa)	Bending moment M (N*m)	Primary bending Pb=M/W (MPa)	Pm+Pb (MPa)	1.5*Sm (MPa)	Safety margin 1-(Pm+Pb)/(1.5*Sm)
III	III.25	7.27E+02	0.4	5.20E+03	122.1	122.5	190.5	0.36
IV	IV.13	1.27E+04	6.7	1.46E+04	342.1	348.8	409.5	0.15

Table 6
Maximum deformations in normal operation.

Location	Direction	Max. displacement (mm)	Load
Launcher	Axial	3.16	Gravity/5 °C
	Transverse	3.74	Gravity/5 °C
Receiver	Axial	2.46	Gravity/5 °C
	Transverse	1.70	Gravity/35 °C

Table 7
Maximum displacements per type of sliding joint in LOCA and Fire events.

Sliding joint range		Max. displacement (mm)	Location
Launcher	25mm	20.49	SJ#8 (Fig. 11)
	50mm	48.50	SJ#10 (Fig. 11)
Receiver	20mm	18.44	SJ#5 (Fig. 12)
	40mm	36.67	SJ#2 (Fig. 13)

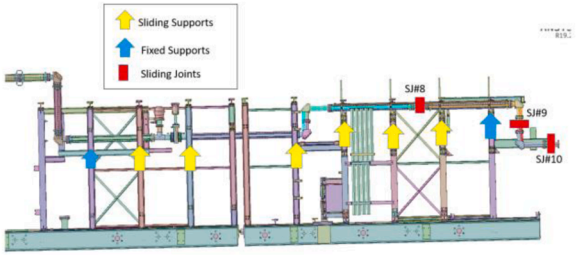

Fig. 11. Distribution of the Launcher sliding joints in the PCSS and ISS, and location of SJ#8 and SJ#10.

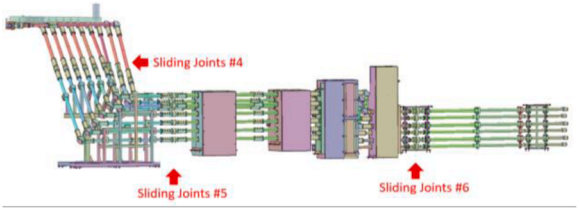

Fig. 12. Distribution of the Receiver sliding joints in the PCSS and ISS, and location of SJ#5.

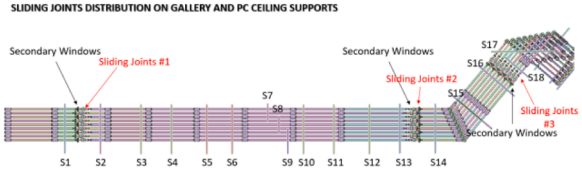

Fig. 13. Distribution of the Receiver sliding joints in the Gallery and PC ceiling, and location of SJ#2.

the CTS Launcher TL ex-vessel components, at the Preliminary design stage. Bolts, pins and welds will be analyzed when they are defined in the later stages of the CTS design.

Primary stresses meet the RCC-MR structural criteria. Therefore, the structural integrity of the TLs for P-type damage is assured.

Natural frequencies calculated in the Modal analysis show that there are not clearly dominant modes of vibration, as the CTS Layout distribution gives rise to several local modes.

Thermomechanical deformations in normal operation meet the system requirements. Deformations in extreme conditions like LOCA or Fire event are proved to be absorbed by the sliding joints defined for the Launcher and Receiver TLs.

Boundary conditions for supports and TLS have been optimized during the structural analysis in an iterative process, also checking that there are not excessive loads induced on the TLs during fire events.

In summary, the analyses performed and reported in this paper confirm that the preliminary design of the CTS Ex-port plug TLs is valid to continue with the final design stage.

Disclaimer

The work leading to this publication has been partially funded by ITER Organization under Implementing Agreement No. 1 (ITER ref. IO/20/CT/4,300,002,249). The views and opinions expressed herein do not necessarily reflect those of the ITER Organization.

Declaration of Competing Interest

The authors declare that they have no known competing financial interests or personal relationships that could have appeared to influence the work reported in this paper.

Data availability

The authors do not have permission to share data.

References

[1] S.B. Korsholm, et al., Design and development of the ITER CTS diagnostic, EPJ Web Conf. 203 (2019) 03002, https://doi.org/10.1051/epjconf/201920303002.
[2] R.A. Olstad, et al., ECH MW-level CW transmission line components suitable for ITER, Fusion Eng. Des. 74 (Issues 1–4) (2005) 331–335, https://doi.org/10.1016/j.fusengdes.2005.06.070. VolNovember.
[3] R.W. Callis, et al., Design and testing of ITER ECH & CD transmission line components, Fusion Eng. Des. 84 (Issues 2–6) (2009) 526–529, https://doi.org/10.1016/j.fusengdes.2008.11.096. June.
[4] D. Strauss, et al., Preliminary design of the ITER ECH upper launcher, Fusion Eng. Des. 88 (2013) 2761–2766, https://doi.org/10.1016/j.fusengdes.2013.03.040. November.
[5] P. Santos Silva, et al., Design concept and thermal-structural analysis of a high power reflective mm-wave optical mirror (M2) for the ITER ECH-UL, Fusion Eng. Des. 146-A (2019) 618–621, https://doi.org/10.1016/j.fusengdes.2019.01.037. September.
[6] 55.C7.C0/D0 - SLS for components in B13 (ITER_D_6WGDBH_v1.2). https://user.iter.org/?uid=6WGDBH (2023).
[7] 55.C7.C0/D0 - SLS for components in Gallery (ITER_D_6WG9XA_v1.1). https://user.iter.org/?uid=6WG9XA.

[8] 55.C7.C0/D0 - SLS for components in interspace and port cell area (ITER_D_6WFY3N_v1.1). https://user.iter.org/?uid=6WFY3N.
[9] 55.C7.C0/D0 - SLS for components in B74 (ITER_D_6WGJ9S_v1.2) https://user.iter.org/?uid=6WGJ9S.
[10] 55.C7.C0/D0 - SLS basic information record in gallery (ITER_D_6CWCAU_v1.3) https://user.iter.org/?uid=6CWCAU.
[11] 55.C7.C0/D0 - SLS basic information record in interspace and port cell area (ITER_D_6CVDM3_v1.2) https://user.iter.org/?uid=6CVDM3.
[12] 55.C7.C0/D0 - SLS basic information record in B74 (ITER_D_6CWWP5_v1.1). https://user.iter.org/?uid=6CWWP5.
[13] AFCEN. Design and construction rules for mechanical components of nuclear installations. RCC-MR 2007 Section1, subsection z Appendix A3.
[14] R. Reichle et al., SRD-55 (Diagnostics) from DOORS ITER_D_28B39L v5.5, November 2021, ITER private communication.
[15] R. Roccella et al., Magnetic field maps (MFM) in ITER_D_XMCQMZ v1.2, May 2019, ITER private communication.
[16] S. Iglesias et al., EM analysis of ISS ITER_D_4FYSR5 v1.0, November 2020, ITER private communication.